BioEnergy Research
https://doi.org/10.1007/s12155-021-10355-4

NDP-Sugar Pathways Overview of *Spirodela polyrhiza* and Their Relevance for Bioenergy and Biorefinery

Débora Pagliuso[1] · Bruno Viana Navarro[1] · Adriana Grandis[1] · Marcelo M. Zerillo[2] · Eric Lam[3] · Marcos Silveira Buckeridge[1]

Received: 2 August 2021 / Accepted: 26 October 2021

Abstract
Duckweeds are fast-growing aquatic plants suitable for bioenergy due to fermentable-rich biomass with low lignin and unique cell wall. The plant cell wall is built from pathways of nucleotide sugar genes that culminate in cell wall synthesis and deposition. Therefore, understanding these pathways by mapping the genes involved and their expression would be necessary for developing tools to improve bioenergy production. In this work, the genes associated with the NDP-sugar pathway (de novo and *salvage*) were mapped and correlated to the chemical characterization of the giant duckweed (*Spirodela polyrhiza*) cell wall. This plant biomass has been characterized as having 3% starch, 49% soluble sugars, 40% cell wall, and 8% non-measured compounds. The cell walls are synthesized by the NDP-sugar pathway and represent a significant carbon sink. This sink results from the action of proteins encoded by 190 orthologs of the 38 targets of the NDP-sugar pathway, of which 49 are starch and sucrose-related, 54 pectins-related, 65 hemicellulose-related, and 23 cellulose-related. Chemical analysis of the cell wall revealed 49% pectins, 23% hemicellulose, and 10% cellulose. These carbohydrates can potentially provide biorefinery as adjuvants, cosmetics, food additives, stabilizers, gelling agents, and principally as biofuels.

Keywords Duckweed · Cell wall · Polysaccharides · Biofuels · Carbohydrate synthesis

Introduction

After the carbon is assimilated through photosynthesis, it is stored as soluble sugars (e.g., sucrose), starch, and cell walls through a series of metabolic transformations. Carbon can be stored in different forms and proportions depending on the species and the tissue. However, in most cases, plant tissues will accumulate the majority of the carbon as cell walls. Thus, most of the energy stored as chemical bonds within biomass is found in the plant cell walls. As a result, a deep understanding of carbon metabolism will be necessary to control the distribution of compounds that hold bioenergy in the form of carbohydrates (the primary polymers in plant cell walls).

Plant cells are surrounded by an encoded polymeric structure composed of polysaccharides (pectins, hemicellulose, and cellulose), proteins, and phenolic compounds. This composite confers physical, chemical, and mechanical protection throughout plant growth and development [1, 2]. Cell wall polysaccharides are organized as a core of cellulose microfibrils, surrounded by hemicellulose and phenolic compounds, and immersed in a pectin matrix [2]. The cellulose microfibrils are formed by 1,4-β-glucan chains and represent 40% of the cell wall composition in terrestrial plants [3]. The polysaccharides attached to the cellulose surface represent 30% of the cell wall. They are hemicelluloses, a class of 1,4-linked backbone polymers including xyloglucans, heteroxylans, and heteromannans [3]. The pectins are the most complex polymers, composed mainly of galacturonic acids (70%), which are linked at *O*-1 and *O*-4 to form homogalacturonans, rhamnogalacturonans, xylogalacturonans, and apiogalacturonans [4]. Plant cell wall is generally conserved among species, despite slight modifications depending on the tissues [1]. Nevertheless, it has been recently found that

✉ Marcos Silveira Buckeridge
msbuck@usp.br

[1] Laboratory of Plant Physiological Ecology, Department of Botany, Institute of Biosciences, University of São Paulo, São Paulo, Brazil

[2] GaTE Lab, Department of Botany, Institute of Biosciences, University of São Paulo, São Paulo, Brazil

[3] Department of Plant Biology and Pathology, Rutgers, The State University of New Jersey, New Brunswick, NJ, USA

Published online: 10 January 2022

the cell walls of duckweeds display remarkable plasticity [7]. Therefore, these plants can be an interesting model for evaluating how carbon distribution is controlled.

Duckweeds are the smallest flowering aquatic plants with fast growth [5]. These plants display a unique cell wall rich in pectins and lacking lignin [6, 7]. The unusual chemical composition of duckweed cell walls and the low recalcitrance to hydrolysis make it suitable for bioenergy production, such as ethanol [6, 8, 9]. Furthermore, the high proportion of apiogalacturonans (their primary pectin polymer) makes these plants suitable for use as adjuvants [10] or as cosmetic and dermatological preparations for skincare [11]. Moreover, the fast growth capacity (up to 100-ton dry matter ha^{-1} $year^{-1}$) and their ability of water clean-up make duckweed a sustainable feedstock [12].

The cell wall is one of the most significant carbon sinks (biomass sources), making sugars available for feedstock and industrial applications such as bioenergy, cosmetology, pharmaceutical, and food inputs [13]. Polysaccharide synthesis requires nucleotide diphosphate (NDP)-sugars synthesized by condensed triose-phosphate from photosynthesis [13]. NDP-sugars can also be the product of hydrolysis of translocated sucrose or sugars released from storage polymers, glycoproteins, glycolipids, and polysaccharides recycling during primary and secondary walls restructuring [14]. The action of several glycosyltransferases performs the chemical linkages of the polymers chains [4]. These reactions occur in the Golgi apparatus, and the polymers produced (hemicellulose and pectins) are further exported to the cell wall space by the membrane by vesicles [4, 13]. One exception is cellulose, synthesized at the plasma membrane, where cellulose synthases are assembled as complexes of six proteins named rosettes (CESA; EC 2.4.1.12) [14]. The wall synthesis requires UDP-glucose as a central precursor, which is synthesized by UDP-glucose-pyrophosphorylase (UGP, EC 2.7.7.9), sucrose synthase (SUSY, EC 2.4.1.13), and invertase (INV, EC 3.2.1.26) [13] (Fig. 1). UDP-glucose is also the precursor of UDP-rhamnose (UDP-Rha), UDP-galactose (UDP-Gal), and UDP-glucuronate (UDP-GlcA), hence involved not only in cellulose but also in hemicelluloses and pectin syntheses [14]. The only NDP-sugars that are not derived from the UDP-glucose are GDP-mannose

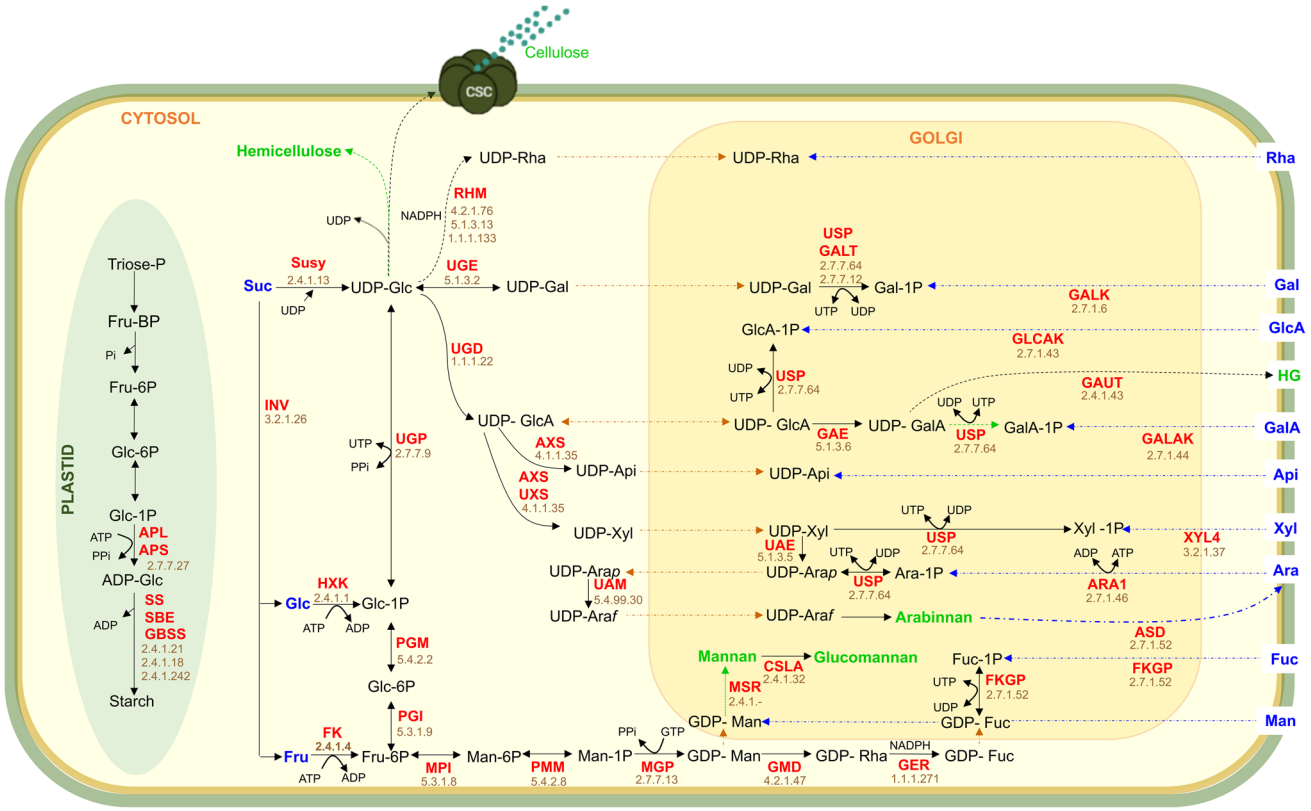

Fig. 1 Starch synthesis, *de novo* and *salvage* pathways of NDP-sugars. Sugars are shown in blue and their precursor in black. The genes encode the enzymes that synthetize the NDP-sugar are shown in black and red. The ones in red had their expression measured in this work, whereas the black did not. Some cell wall polysaccharides are shown in green. Dashed lines in black indicate multi-steps to generate the product indicated by the arrowhead. Dashed lines in green indicate unresolved pathways. Dashed lines in orange-brown indicate transporters to the Golgi complex. Dashed blue lines indicate the reactions of the *salvage* pathway. The NDP-sugars are the building blocks for the monosaccharides that are arranged in cell wall polymers. For detail of the pathway and abbreviations, please see Supplemental Box 1

(GDP-Man) and GDP-fucose (GDP-Fuc) [15], which are synthesized from fructose-6-phosphate and are part of the mannan type of hemicellulose and side branching of xyloglucan and pectins (Fig. 1).

The cell wall production involve six steps: synthesis of nucleotide-sugar and monolignols (i); synthesis of oligomers and polysaccharides at the plasma membrane and ER-Golgi apparatus (ii); the targeting and secretion of the Golgi-derivate materials (iii); the assembly and architectural patterning of polymers (iv); dynamic rearrangement during cell growth and differentiation (v); wall disassembly and catabolism of the spent polymers (vi) [16]. The mentionated steps are fundamental to address the final matrix, and each of them is complex and lack of complete understanding [16]. The first stage is crucial for monosaccharides synthesis that are the building blocks of the wall polysaccharides. Therefore, understanding the carbon partition to the cell wall regarding the first step may enhance modulation sets that improve industrial applications.

The present work highlights the carbon pathway genes in the giant duckweed *Spirodela polyrhiza*. Some of the genes from the *de novo* and *salvage* NDP-sugar pathway were mapped. Their expression and the cell wall chemical characterization were used to produce an overview of the carbon pathway and its possible applications. It is expected that future work could be performed that leads to plants with engineered cell walls for different applications of duckweed cell walls towards bioenergy and biorefinery.

Material and Methods

Plant Material

The *S. polyrhiza* clones 9509 and 7498, originally from Germany (Lotschen, Stradtroda) and USA (North Carolina, Durham), respectively, were acquired from Rutgers Duckweed Stock Cooperative (RDSC). The plants were grown axenically in 250 mL of ½ Schenck-Hildebrandt (300 mg L^{-1} $(NH_4)_3PO_4$; 5 mg L^{-1} H_3BO_3; 151 mg L^{-1} $CaCl_2$; 0.1 mg L^{-1} $CoCl_{2*}6H2O$; 0.2 mg L^{-1} $Cu.SO_{4*}5H_2O$; 20 mg L^{-1} Na_2.EDTA; 15 mg L^{-1} $FeSO_{4*}7H_2O$; 195.4 mg L^{-1} $MgSO_4$; 10 mg L^{-1} $MnSO_{4*}H_2O$; 0.1 mg L^{-1} $H_2MoO_{3*}2H_2O$; 1 mg L^{-1} KI; 2500 mg L^{-1} KNO_3; and 1 mg L^{-1} $ZnSO_{4*}7H_2O$—Sigma-Aldrich®) medium supplemented with 0.5% sucrose and maintained at 25 °C in a 16-h light/8-h dark photoperiod with a light intensity of 20 µmols m^{-2} s^{-1}.

Non-structural Carbohydrates

Plants were harvested after 10–15 days of cultivation, freeze-dried, and ground in GenoGrinder2010 (Spex®, USA). Five hundred milligrams of each milled sample was extracted 4 times with 25 mL of 80% ethanol (v/v) at 80 °C for 20 min. The supernatants containing soluble sugars and other soluble compounds were recovered, vacuum dried (ThermoScientific® Savant SC 250 EXP), and resuspended in 1 mL of water and 1 mL of chloroform. The residue (Alcohol Insoluble Residue-AIR) was dried at 40 °C and reserved. The soluble sugars were analyzed by High-Performance Anion Exchange Chromatography with Pulsed Amperometric Detection (HPAEC-PAD) in a Dionex® system (ICS 3,000), using a CarboPac PA1 column eluted with 150 µM sodium hydroxide in an isocratic run of 27 min [7].

The AIR dried-residue from the ethanolic extractions was treated with 120 U/mL of α-amylase (E.C. 3.2.1.1) (Megazyme® Inc., Australia) diluted in 10 mM of 3-(N-Morpholino)propane sulfonic acid (MOPS) buffer pH 6.5 at 75 °C for 1 h for starch removal. For the starch determination, the reactions followed with the addition of 30 U mL^{-1} of amyloglucosidase (E.C. 3.2.1.3) (Megazyme® Inc., Australia) diluted in 100 mM sodium acetate pH 4.5 at 50 °C for 1 h. For the colorimetric assay, 5 µL of the hydrolyzed material was diluted in 45 µL of deionized water and reacted with 250 µL of glucose oxidase (1100 U mL^{-1}), peroxidase (700 U mL^{-1}), 4-aminoantipirin (290 µmol L^{-1}), and 50 mM of phenol at pH 7.5 for 15 min at 30 °C. The reactions were read at 490-nm spectrophotometer (MultiSkan FC, ThermoScientific®), and the quantification was performed with a calibration curve of 0.02–0.2 mg L^{-1} glucose (Sigma®). The final residue (de-starched AIR – cell wall) was recovered, washed in ethanol, frozen, and freeze-dried.

Cell Wall Fractionation and Neutral Monosaccharides Quantification

The cell walls were submitted to several extractions to solubilize each polysaccharide class. First, the material was extracted three times with 25 mL of 0.5 M ammonium oxalate (pH 7.0) at 80 °C for 1 h each with continuous stirring to remove pectins. The supernatants were recovered by centrifugation, and the oxalate-extracted cell wall residues were extracted with 25 mL of 3% (w/v) of sodium chlorite in 0.3% (v/v) acetic acid for lignin removal. The supernatants were also recovered, and the hemicelluloses from the sodium chlorite in cell wall residues were extracted three times with 25 mL each of 0.1, 1, and 4 M NaOH supplemented with 3 mg mL^{-1} of sodium borohydride at room temperature for 1 h. All the supernatants and the residue were recovered, neutralized, dialyzed, and freeze-dried. The mass balance and fractionation yield were calculated gravimetrically.

The recovered cell wall fractions were hydrolyzed with 1.5 mL of 2 M trifluoroacetic acid (TFA) for 1 h at 100 °C with continuous stirring. The vacuum-dried reactions were resuspended in 1 mL MiliQ water and filtrated on 0.22 µm (Merck Millipore®). The monosaccharides were analyzed by HPAEC-PAD into a CarboPac SA10 column (ICS 5,000

system, Dionex-Thermo®) eluted isocratically with 99.2% water and 0.8% (v/v) 150 mM NaOH with a flux 1 mL min^{-1} with 500 mM NaOH post-column base with a flux of 0.5 mL min^{-1}. The standard curve was used to calculate the concentration of each monosaccharide in the fractionation samples.

S. polyrhiza 9509 Gene Prediction

The genome of *S. polyrhiza* 9509 has been previously sequenced at the chromosome level (with gaps) (GenBank assembly accession GCA_001981405.1, loci CP019093.1—CP019112.1), but gene annotation is not available on Phytozome or elsewhere. To associate the NDP-sugar genes of *A. thaliana* to potential orthologous in 9509 (as described below), it was performed *an ab initio* gene prediction of this strain. The Augustus prediction tool (version 3.3.2) (http://augustus.gobics.de/) was set with the default parameters and trained on the *Arabidopsis thaliana* gene model (species = arabidopsis), which is the closest to *Spirodela*, among the plants contained in the tool's data set. The predicted genes/proteins were validated in further analyses, as described below. For functional annotation, the predicted proteins were subjected to a BLASTp search against the NCBI non-redundant (nr) database, InterProScan search, and Gene Ontology mapping by using Blast2GO v4. Only cutoff e-value $< 1.10^{-5}$ were considered, and Fisher's exact test was used to detect GO terms enrichment (with p-value ≤ 0.05).

NDP-Sugar Genes Screening and Query Selection

Based on information of amino- and NDP-sugar metabolisms available at the Kyoto Encyclopedia of Genes and Genomes (KEGG) Pathway (map00520) and data from Verbančič et al. [13], it was established a comprehensive pathway depicting the enzymes, target genes, and sugar products related to cell wall metabolism (Fig. 1). The sequences of related genes and predicted proteins from *A. thaliana* were used as queries on a sequence similarity search against the genomes of *S. polyrhiza* 9509 and 7498 (Supplemental Table 1). Comparison with the 7498 genomes was performed by using the tBlastN tool (E-value $> e^{-10}$) on the Phytozome *v*12.1.6 website (https://phytozome.jgi.doe.gov/), or by using local BlastP against the predicted-proteins database of the 9509 genome since the latter was not available on Phytozome. Sequences with coverage $\geq 70\%$ and a similarity $\geq 80\%$ were retrieved and considered orthologs (Supplemental Table 1). The homologous protein sequences obtained were annotated and classified using HMMER Scan (https://www.ebi.ac.uk/Tools/hmmer/) (Supplemental Table 2). Multiple alignments were performed using Clustal Omega Program (Bioedit®) to identify possible introns and conserved regions, and the latter were selected for primer design. The physical distribution among the 20 chromosomes was determined based on data retrieved from Phytozome, and the chromosomal ideogram of the NDP-sugar pathway genes evaluated in the present study was designed by PhenoGram tool software (https://ritchielab.org/software/phenogram-downloads), available online.

The sugar and cell wall–related genes of the 9509 genome were further compared with the Reference Sequence (RefSeq) database of NCBI by BlastX (E-value $> e^{-10}$) and with the InterPro database for the search of functional domains with protein families associated with sugar metabolism.

Candidate Reference Genes Selection

Thirteen reference genes were selected as normalizers candidates: *60S ribosomal protein L18A-A (60S)*, *Actin-related protein (ARP7)*, *cyclophilin (CYP)*, *Elongation factor 1-α (EF1)*, *Translational initiation factor 4B (ELF4B)*, *F-box family protein (FBOX)*, *protein phosphatase 2A (PP2A)*, *D1 subunit (PSAB)*, *S24 ribosomal protein (S24)*, *Tubulin α3/α5 chain (TUA)*, *Ubiquitin-conjugating enzyme (UBQ9)*, *Ubiquitin 7 (UBQ7)*, and *Ribosomal RNA small subunit methyltransferase NEP* 1 *(18S)* (Supplemental Table 3). In addition, the annotated genome of *S. polyrhiza* (7498) was analyzed using a blasting program (NCBI®) (https://blast.ncbi.nlm.nih.gov/Blast.cgi), by which the sequences of *A. thaliana* and *Lemna minor* were used as queries as described below for primer design (Supplemental Table 4).

Primer Design

Primers were designed for 38 genes of the NDP-sugar pathway and all the reference gene candidates (Supplemental Table 4), by using Primer-Blast® (NCBI) tool (https://www.ncbi.nlm.nih.gov/tools/primer-blast/), according to MIQE guidelines. Oligo Analyzer Tool® program (Integrated DNA Technologies®) (https://www.idtdna.com/calc/analyzer/) was used to estimate the potential formation of secondary structures in those. Primers targeting *phosphoglucose isomerase* (*SpPGI*), *mannose-6P-isomerase* (*SpMPI*), *phosphomannomutase* (*SpPMM*), *mannose-1P-guanylyltransferase* (*SpGMD*), and *UDP-arabinose-4-epimerase* (*SpUAE*) were designed based exclusively on the *S. polyrhiza* 7498 transcripts. The lyophilized oligonucleotides (DNA Express Brazil® and Exxtend®) were resuspended in Tris 10 mM EDTA 1 mM pH 7.0 (ThermoScientific®), to reach the final concentration of 100 µM, and stored at − 20 °C.

RNA Extraction, DNase Treatment, and cDNA Synthesis

Plant material was harvested after 10 days of cultivation and homogenized in liquid nitrogen. The RNA was extracted

using ReliaPrep™ RNA Tissue Miniprep System (Z6112, Promega®, USA) and followed the DNase treatment as the manufacturer's instructions. RNA quantification and purity were assured using a Nanodrop ND-100 spectrophotometer (Thermo Fischer Scientific), and samples with 260/280 ratios between 1.8 and 2.2 were taken as sufficiently pure. The samples' integrity was also secured by electrophoresis on a 1% agarose gel and stained with SYBR Safe DNA gel stain (1,771,581, Thermo Fischer Scientific, USA). Approximately 1 ug of each RNA sample was reverse transcribed with random hexamers by SuperScript III Reverse Transcriptase (Thermo Fischer Scientific, USA). The cDNA acquired were tested for the absence of genomic DNA with UPD-*apiose/UDP-xylose synthase* (*AXS*) primers (Forward: 5′- GCATCCAGTTCCACCGTCTC -3′; Reverse: 5′- GCA GGGCGTTTCATCTTCTTT -3′).

qRT-PCR Analysis

The relative abundance of target transcripts in *S. polyrhiza* 9505 and 7498 was measured by qRT-PCR analysis using a QuantiStudio 6 Flex Real-Time PCR system (Applied Biosystems by Life Technologies, NY, USA). The PCR reactions were performed with 1.4 µL of cDNA (1:10), 7 µL 2X SYBR Green Master Mix (Applied Biosystems by Life Technologies, NY, USA), and the following cycling conditions: 95 °C for 10 min, 40 cycles of 95 °C for 15 s, 60 °C for 30 s, and 72 °C for 30 s. The amplification of a single product was confirmed by a melting curve analysis (data not shown). After testing the concentrations of 200 nM, 400 nM, and 800 nM of the primer set, it chose 800 nM as the optimal concentration based on the lowest quantification cycle (Cq) values, highest primer efficiency values, and the absence of primer dimers. The Cq values and the efficiency of each primer were determined using LinRegPCR software, and only the genes with transcripts holding Cq values ≤ 35 followed the further analysis (Supplementary Fig. 2).

Consistency and Validation of Reference Genes

The consistency of the candidate reference genes was determined by the statistical approaches of GeNorm v.3.5 software (http://medgen.ugent.be/~jvdesomp/genorm/) and NormFinder software (http://mdl.dk/publicationsnormfinder.htm) (Supplemental Table 4). The relative expression level of the gene *SpAXS* was evaluated in both *S. polyrhiza* lineages to confirm and validate the selected reference genes. The relative expression of *SpAXS* was quantified compared to the average expression, normalized by the highest Cq value of the tested sample, and the Cq values of the target genes were normalized by the geometric average of the reference genes combination (Supplementary Fig. 2).

Data Analysis from Biochemical Evaluation

Five independent replicates were used for the analyses of soluble sugars, starch, cell wall polysaccharide, and gene expression. Data were analyzed by ANOVA one-way ($p < 0.05$) followed by Tukey's test ($p < 0.05$). The analysis was carried out with R version 3.6.1.

Results

Non-structural and Structural Carbohydrates

S. polyrhiza carbohydrates were analyzed as soluble sugars, starch, and cell wall polysaccharides. The soluble sugars and starch constitute the non-structural carbohydrates representing more than half of the biomass (Fig. 2). Thus, the *S. polyrhiza* biomass was determined as 48.9% soluble sugars, 3.3% starch, 39.5% structural carbohydrates (cell walls), and 8.3% other compounds (Fig. 2). When calculated as the percentage of the biomass, the soluble sugars were mainly fructose (20%), followed by sucrose (17%) and glucose (11.7%), and low amounts of raffinose (0.3%).

Regarding the cell walls, 59% were pectins (fractions from extraction with ammonium oxalate and sodium chlorite), 28% hemicelluloses (fractions from extraction with 0.1, 1, and 4 M NaOH), and 13% cellulose (residue) (Table 1). The cell wall fractionation will be described as the mentioned classes (pectin, hemicellulose, and cellulose) within the corresponding fractions summed. The majority of the pectins were composed of apiose (56.5 µg mg^{-1} cell wall—38%), arabinose (23.8 µg mg^{-1} cell wall—16%), and galactose (28.9 µg mg^{-1} cell wall—19.5%), with traces of fucose (2.9 µg mg^{-1} cell wall—2%) (Table 1, AmnOx and Chlorite columns). Xylose (39.1 µg mg^{-1} cell wall—32%), glucose (17.3 µg mg^{-1} cell wall—14%), and galactose (17.2 µg mg^{-1} cell wall—14%) were the main monosaccharides of the hemicellulose fractions, suggesting xylan as the principal hemicellulose followed by xyloglucan in *S. polyrhiza* (Table 1, 0.1 M, 1 M, and 4 M NaOH fractions). The soluble hemicellulose glucomannan was found on the fraction of ammonium oxalate with significant proportions of mannose (6.1 µg mg^{-1} cell wall) and glucose (4.8 µg mg^{-1} cell wall) (Table 1). The residue comprised more than 80% cellulose (151.7 µg mg^{-1} cell wall) (see glucose levels on Residue II in Table 1). The residue II fraction composition also showed small amounts of galactose (6.3 µg mg^{-1} cell wall), xylose (11.8 µg mg^{-1} cell wall), and apiose (5.8 µg mg^{-1} cell wall), suggesting possible crosslinks among apiogalacturonans, galactans, and xyloglucans with the cellulose microfibrils of *S. polyrhiza* (Table 1, residue II fraction).

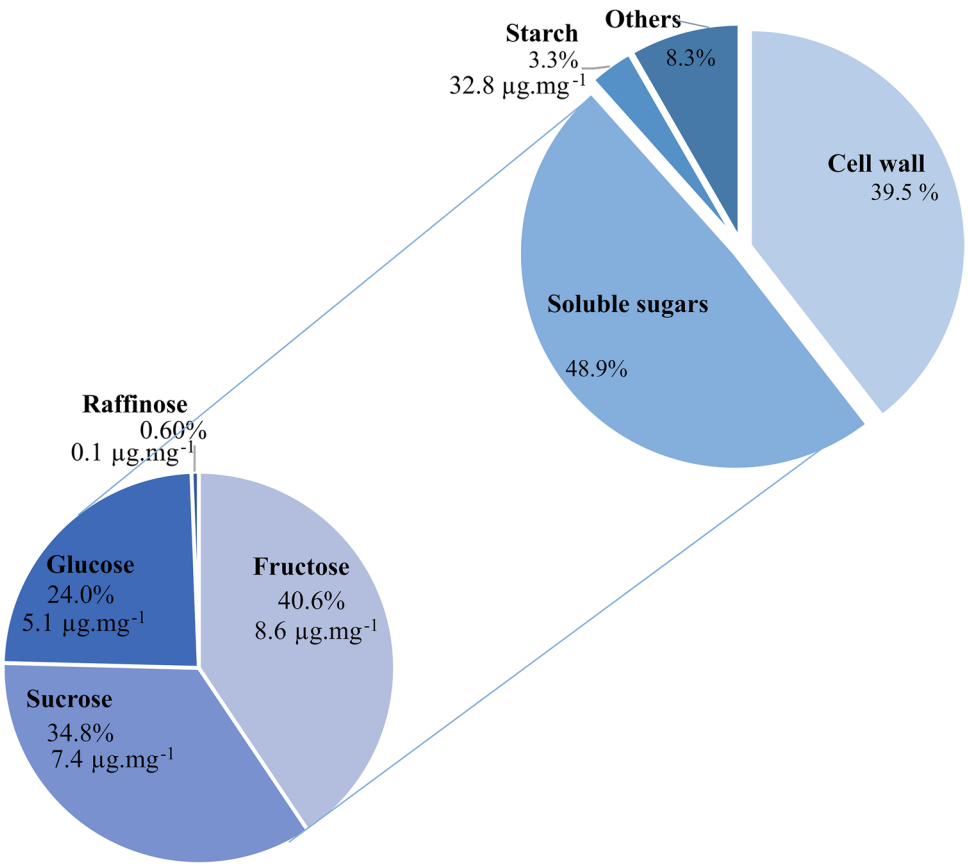

Fig. 2 *S. polyrhiza* biomass composition. This plant biomass was analyzed regarding the soluble sugars content (fructose, sucrose, glucose, and raffinose), starch levels, cell wall proportion, and others. Others represent the biomass lost during the processing, comprehending possibly to secondary metabolites and lipids. All data are represented by the average (n = 5)

Table 1 Cell wall yield and composition of *S. polyrhiza*. A. Yield of cell wall extractions of de-starched alcohol insoluble residues of *S. polyrhiza*. B. The structural carbohydrates show the cell wall composition by monosaccharides hydrolysis with TFA. Despite the monosaccharide's hydrolysis, the residue fraction, main cellulose, was also hydrolyzed with sulfuric acid 72% to prove its nature since TFA cannot hydrolyze cellulose (shown as Residue II). *AIR*, alcohol insoluble residue; *AmnOx*, ammonium oxalate fraction; *chlorite*, sodium chlorite fraction; *0.1–4 M NaOH*, sodium hydroxide fractions, and residue. All data are represented by the average ± standard error of the sugar in µg mg^{-1} dry weight ($n = 5$)

	AIR	AmnOX	Chlorite	0.1 M NaOH	1 M NaOH	4 M NaOH	Residue	Residue II
A. Yield (%)	-	20.37 ± 0.44	38.33 ± 0.96	7.36 ± 0.40	8.71 ± 1.03	12.42 ± .78	12.85 ± 1.10	-
B. Neutral carbohydrates (µg mg^{-1} DW)								
Galactose	74.85 ± 5.19	17.42 ± 0.09	11.53 ± 0.06	10.15 ± 0.04	4.47 ± 0.03	2.58 ± 0.01	7.37 ± 0.07	6.28 ± 0.00
Arabinose	56.01 ± 5.09	10.12 ± 0.05	13.68 ± 0.05	5.35 ± 0.03	1.57 ± 0.02	0.75 ± 0.00	2.21 ± 0.02	1.50 ± 0.00
Xylose	51.93 ± 2.06	6.11 ± 0.03	2.68 ± 0.02	11.35 ± 0.04	18.89 ± 0.17	8.87 ± 0.06	14.50 ± 0.10	11.84 ± 0.01
Apiose	49.81 ± 4.15	44.28 ± 0.18	12.23 ± 0.08	20.80 ± 0.09	6.02 ± 0.03	4.97 ± 0.05	19.64 ± 0.21	5.86 ± 0.01
Mannose	43.92 ± 3.11	6.18 ± 0.05	3.40 ± 0.02	0.09 ± 0.01	0.77 ± 0.00	0.63 ± 0.00	0.87 ± 0.00	3.12 ± 0.01
Rhamnose	28.36 ± 1.70	8.00 ± 0.04	2.46 ± 0.02	3.97 ± 0.01	0.49 ± 0.01	0.57 ± 0.01	2.92 ± 0.03	0.00 ± 0.00
Glucose	11.87 ± 1.34	4.79 ± 0.08	2.33 ± 0.01	2.52 ± 0.01	10.96 ± 0.17	3.81 ± 0.02	7.80 ± 0.07	151.7 ± 0.21
Fucose	7.19 ± 0.55	2.14 ± 0.01	0.90 ± 0.00	1.02 ± 0.00	1.19 ± 0.01	0.62 ± 0.00	1.76 ± 0.02	1.08 ± 0.00

Mapping of Orthologous Sequences Throughout the Chromosomes of S. polyrhiza

Using thirty-seven target genes of *de novo* and *salvage* NDP-sugars pathways and starch synthesis (Fig. 1) of *A. thaliana,* it was retrieved 190 orthologous sequences from *the S. polyrhiza* genome (Figs. 3 and 4, Supplemental Table 1). The recovered sequences had similarities above 70% with queries in public databases (Supplemental Tables 1) and showed conserved protein domains (Supplemental Tables 2).

The recovered genes were divided into the categories that were named: "starch and sucrose metabolism" (*SpSUSY*,

SpINV, *SpFK*, *SpHXK*, *SpPGI*, *SpPGM*, *SpUGP*, *SpAPL*, *SpAPS*, *SpSS*, and *SpSBE* contemplating 49 orthologs), "pectin" (*SpRHM*, *SpUGD*, *SpAXS*, *SpGAE*, *SpGAUT*, *SpGALAK*, *SpGLCAK*, *SpUAE*, *SpUAM*, *SpARA1*, *SpUSP*, *SpUGE*, *SpGALT*, and *SpGALK*—54 orthologs), "hemicellulose" (*SpUXS*, *SpXYL4*, *SpMPI*, *SpPMM*, *SpMGP*, *SpGMD*, *SpGER*, *SpMSR*, *SpCSLA*, *SpFKGP*, and *SpASD*—65 orthologs), and "cellulose" (*SpCESA*, 23 orthologs) (Figs. 1 and 3). The distribution of the selected genes of this work, which focuses on the carbon pathways that lead to storage (starch and sucrose) or structure (cell walls), tends to have a higher number of genes in the chromosomes 1 and 2 (24 and 22 genes, respectively) that are the largest ones (14.77 and 11.37 Mb) (Figs. 3 and 4). The other chromosomes (3, 4, 5, 8, 9, 13, and 15—that have ~ 7.7 Mb) display a range between 7 and 15 genes compared to the rest (chromosomes 6, 7, 10, 12, 14, 16, 17, 18, 19 and 20—that have ~ 5.3 Mb). Thus, it can be said that some carbon pathways genes could be differentially partitioned in the genome of *S. polyrhiza*. The size of the chromosomes is not related to the occurrence of genes, suggesting that other factors are associated with the topology of the carbon pathways genes in the genome of *S. polyrhiza*.

When analyzed according to metabolic pathways (Fig. 1) that lead to the formation of non-structural sugars (starch, sucrose, and monosaccharides) and structural cell wall carbohydrate polymers (pectin, hemicellulose, and cellulose), the gene distribution varies according to the category

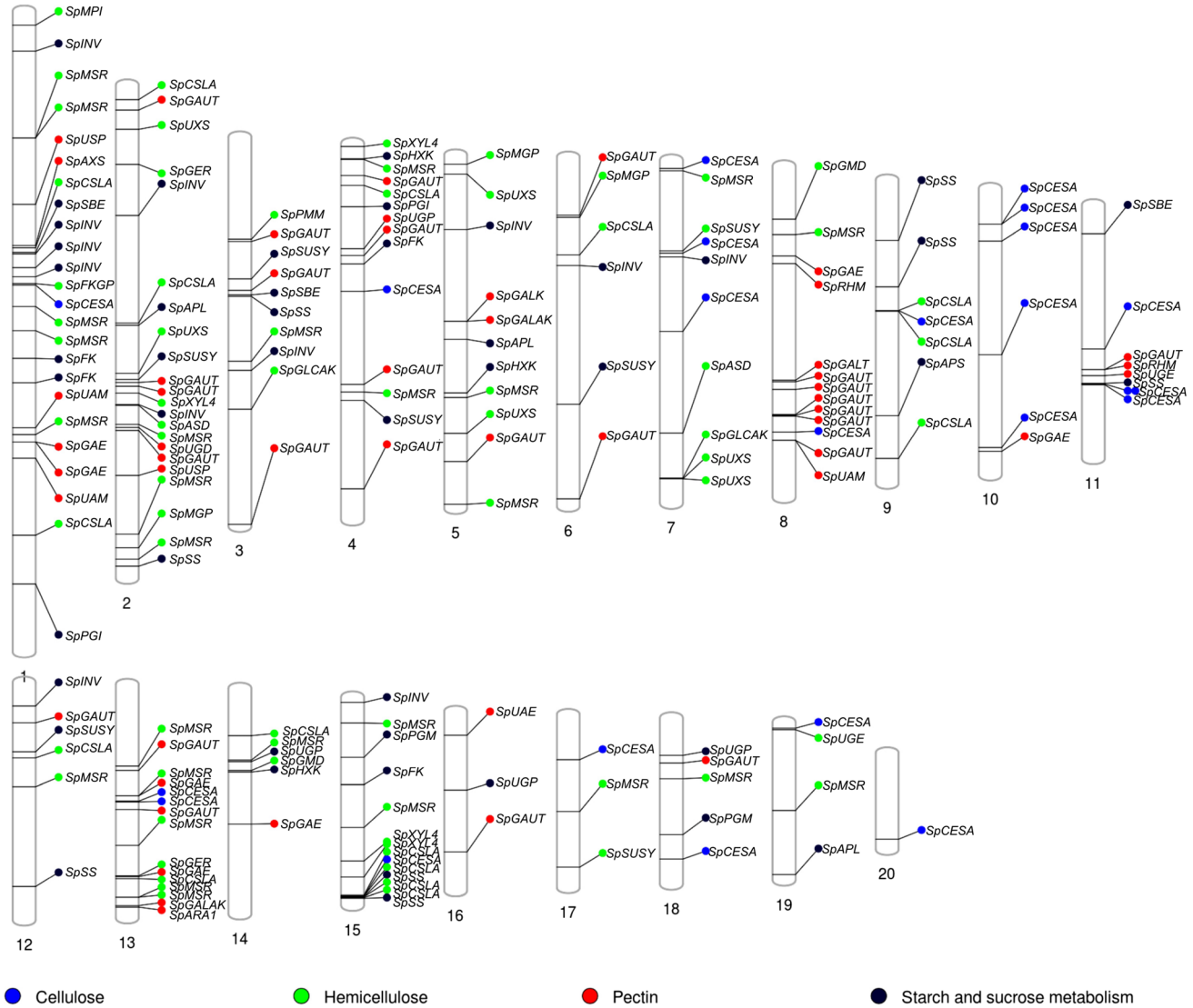

Fig. 3 Chromosome's ideogram of the nucleotide-sugar pathway genes evaluated in the present study. *S. polyrhiza* has 20 chromosomes The colors on the chromosomes represent each class of polysaccharide or its involvement on the pathway, being blue for cellulose, green hemicelluloses, red for pectin, and black for starch and sucrose metabolism. For gene names, see Fig. 1 and Supplemental Table 1

Chromosome number	Number of genes	Starch and sucrose metabolism	Pectin	Hemicellulose	Cellulose
1	24	8	6	9	1
2	22	5	6	11	0
3	10	4	4	2	0
4	14	4	5	4	1
5	11	3	3	5	0
6	7	3	2	2	0
7	10	2	1	4	3
8	13	0	10	2	1
9	7	3	0	3	1
10	6	0	1	0	5
11	9	2	3	0	4
12	6	3	1	2	0
13	15	0	6	7	2
14	6	2	1	3	0
15	14	5	0	8	1
16	3	1	2	0	0
17	3	1	0	1	1
18	5	2	1	1	1
19	4	1	1	1	1
20	1	0	0	0	1
TOTAL	190	49	53	65	23
	%	25.8	27.9	34.2	12.1

Fig. 4 Distribution of genes throughout the chromosomes in the genome of *S. polyrhiza*. Heatmap of the number of genes in each chromosome of *S. polyrhiza* divided into the categories "sucrose and starch metabolism," "pectin," "hemicellulose," and "cellulose." The darker the blue, the higher the number of genes in the chromosome

(Figs. 3 and 4). Starch-related genes are more randomly distributed throughout the chromosomes 1–3, 5, 9, 11–13, 15, and 19. Pectin-related genes (a total of 54 orthologs) display a more concentrated group in chromosomes 1–5, 8, and 13, with more than 70% of the category's genes. The rest of the chromosomes, 4 (8.6 Mb), 6 (8 Mb), 7 (7.9 Mb), 10 (6.6 Mb), 14 (5.6 Mb), 16 (4.45 Mb), and 18 (4.13 Mb), showed a lower number of genes. For hemicelluloses (65 orthologs), some chromosomes display many genes (1, 2, 13, and 15), with 50% of them in the category. Besides, hemicellulose-related orthologs are not found in chromosomes 10, 11, 16, and 20. Regarding cellulose, approximately 50% of the genes are in chromosomes 7, 10, and 11 (Figs. 3 and 4).

Efficiency and Specificity of Primers and qRT-PCR Amplification

The efficiency and specificity of the primers were tested by qRT-PCR to quantify the relative expression levels of the target genes. They presented values of quantification cycle (Cq) ≤ 35, with reactions that reached the plateau phase. The amplitude of the Cq of the evaluated genes is shown in Supplemental Fig. 2, ranging from 14 to 35 cycles. Among the genes involved in cell wall synthesis, the Cq values in more than 50% of the tested genes were greater than 30 cycles, with *UDP-apiose/UDP-xylose synthase* (*SpAXS)* (22.5 ± 0.1) having the lower Cq-value and *UDP-glucuronate decarboxylase* (*SpUXS3)* (35.0 ± 0.1) the higher Cq-value (Supplemental Fig. 2).

Expression Levels of NDP-Sugars and Related Genes

The relative gene expression levels of the NDP-sugar pathway targets were normalized to that of the *SpARF7* and *SpPP2A* genes (Supplemental Table 4). The expression range of the evaluated targets was 0.5–1.4. Therefore, three levels were established, from 0.5 to 0.8 as low, 0.81–1.1 as medium, and 1.11–1.4 as high.

Out of the 190 NDP-sugar orthologs, 29 targets and 38 orthologs were selected for expression evaluation by qRT-PCR analysis (Table 2). These were the ones that successfully amplified the expected target genes. The expression of *sucrose synthase* (*SpSUSY*), *invertase* (*SpINV*), *hexokinase* (*SpHXK*), and *fructokinase* (*SpFK*) denote anabolic activities that lead to the synthesis of starch and monosaccharides (Fig. 1 and Table 2). Among these, *SpINV* showed the lowest expression value, while other target genes of sugar metabolism ranged from 0.62 to 0.74 (Table 2). The synthesis of starch occurs through the ADP-Glucose pathway (Fig. 1), which involves the *ADP-Glucose pyrophosphorylase* (encoded by *APL* and *APS*), *starch synthase* (*SS*), *α-glucan-branching enzyme* (*SBE*), *granule-bound starch synthase* (*GBSS*). These targets showed a medium expression level when compared to sucrose-related genes (Table 2).

Table 2 Heatmap of selected NDP-sugars pathway associated genes in *S. polyrhiza*. The map was generated by a comparison of all evaluated sugars against themselves. Expression levels in all samples analyzed were normalized to the reference genes ARF7 and PP2A ($n=5$)

	Gene abreviation	Expression level	Gene name	Gene function
Starch and sucrose metabolism	*SBE*	0.90	Starch branching enzyme	Performs branching of starch
	SS2	0.87	Starch synthase	Synthesizes the starch main chan
	APL	0.86	Glucose-1P-adenyltransferase	Converts Glc-1P to ADP-Glc, which is the substrate for starch synthesis
	SUSY1	0.74	Sucrose synthase	Produces UDP-Glucose, the basis of all cell wall polysaccharides except for mannans
	SS1	0.74	Starch synthase	Synthesizes starch main chain
	HXK	0.72	Hexokinase	Produces glucose-6P that is related to starch and cell wall synthesis
	UGP2	0.72	UDP-glucose pyrophosphorylase	Converts UDP-Glc into Glc-1P, determining the pathways of starch or cell wall syntheses
	FK	0.70	Fructokinase	Converts Fructose into Fru-6P which will be substrate for mannan or other cell wall/starch polymers syntheses
	UGP1	0.69	UDP-glucose pyrophosphorylase	Converts UDP-Glc into Glc-1P, determining the pathways of starch or cell wall syntheses
	PGI	0.63	Phosphoglucose-isomerase	Converts Fru-6P to Glc-6P, determining direction towards starch and other cell wall polymers except for mannan
	SUSY2	0.62	Sucrose synthase	Produces UDP-Glucose, the basis of all cell wall polysaccharides except for mannans
	INV	0.52	Invertase	Hydrolyzes sucrose into glucose na fructose, leading to Glc-6P and Fru-6P respectively
Pectins	*GAUT1*	1.37	α-1,4-galacturonosyltransferase	Polymerises the main chain of pectins (homogalacturonnan)
	UGE	1.20	UDP-glucose-4-epimerase	Converts UDP-Glc into UDP-galactose, determining rhamnogalacturonan, galactomannan, xyloglucan, and galactans
	USP	1.05	UDP-sugar-pyrophosphorylase	Converts UDP-GlcA into GlcA-1P, determining rhamnogalacturonan II and glucuronoarabinoxylan syntheses
	RHM	0.92	Rhamnose biosynthesis enzyme	Converts UDP-Glc into UDP-Rham, determining the pathway towards pectin synthesis (Rhamnogalacturonans)
	GAUT2	0.89	α-1,4-galacturonosyltransferase	Polymerises the main chain of pectins (homogalacturonnan)
	UAE	0.89	UDP-arabinose-4-epimerase	Converts UDP-Xyl into UDP-Arap, determining arabinan synthesis and contributing to arabinoxylan and xyloglccan syntheses
	GAUT3	0.84	α-1,4-galacturonosyltransferase	Polymerises the main chain of pectins (homogalacturonnan)
	ARA1	0.83	Arabinokinase	Converts Ara-1P into arabinose that is used for polymerization of chanis of arabinan and branches of arabinoxylan and xyloglucan
	UAM	0.82	UDP-arabinopyranose-mutase	Converts UDP-Arap into UDP-Araf, determining the pathway towards arabainan synthesis
	GALAK2	0.81	Galacturonokinase	Converts UDP-GalA into GalA-1P determining the synthesis of homogalacturonan
	AXS	0.76	UDP-apiose/UDP-xylose synthase	Converts UDP-GlcA into UDP-Api, determining the pathway of apiogalacturonan and rhamnogalacturonan II
	GALAK1	0.67	Galacturonokinase	Converts UDP-GalA into GalA-1P determining the synthesis of homogalacturonan
	UGD	0.65	UDP-glucose-6-dehydrogenase	Converts UDP-Glc into UDP-GlcA, determining the pathways of several pectin and hemicellulosic polymers
	GLCAK	0.54	Glucuronokinase	Converts UDP-GlcA into GlcA-1P, determining rhamnogalacturonan II and glucuronoarabinoxylan syntheses
Hemicelluloses	*CSLA*	1.30	Glucomannan-4β-mannosyltransferase	Polymerizes the main chain of mannan
	GER	1.03	GDP-fucose synthase	Converts GDP-man into GDP-Fuc, contributing to the structure of xyloglucan and pectins
	MP1	0.90	Mannose-6P-isomerase	Converts Fru-6P tinto Man-6P, determining the pathway towards mannan and glycoprotein synthesis
	UXS 2	0.86	UDP-glucuronate-decarboxylase	Converts UDP-GlcA into UDP-Xyl determining the synthesis of xylans, arabinoxylans and xyloglucan
	UXS 4	0.86	UDP-glucuronate-decarboxylase	Converts UDP-GlcA into UDP-Xyl determining the synthesis of xylans, arabinoxylans and xyloglucan
	XYL4	0.84	1,4-β-xylanase	Converts UDP-Xyl into xylose that is incorported by CSLD5 into the xylan polymer
	UXS 3	0.76	UDP-glucuronate-decarboxylase	Converts UDP-GlcA into UDP-Xyl determining the synthesis of xylans, arabinoxylans and xyloglucan
	MGP	0.74	Mannose-1P-guanylyltransferase	Converts Man-1P into GDP-Man, determining the pathway towards mannan and glycoprotein synthesis
	FKGP	0.73	Fucokinase	Converts GDP-Fucose into fucose, contributing the branching of xyloglucan and pectins
	GMD	0.72	GDP-mannose-4,6-dehydratase	Converts GDP-Man into mannose, determining the pathway towards mannan and glycoproein synthesis
	UXS 1	0.69	UDP-glucuronate-decarboxylase	Converts UDP-GlcA into UDP-Xyl determining the synthesis of xylans, arabinoxylans and xyloglucan
	PMM	0.67	Phosphomannomutase	Converts Man-6P into Man-1P, determining the pathway towards mannan and glycoprotein synthesis

However, the high level of 1,6-α-glucan branching enzyme (*SpSBE*—0.9) might indicate that the starch present in *S. polyrhiza* is highly branched. The starch synthesis pathway in duckweeds has particular importance due to the modulation's flexibility for starch accumulation depending on photosynthesis activity.

Pectins have the most complex structure among the cell wall polysaccharides, being composed of several monosaccharides. Therefore, the evaluated expression levels likely associated with pectins should be analyzed carefully due to the co-existence of the same sugars in pectin and hemicelluloses. Pectins' scaffold has the highest transcript levels (*α-1,4- galacturonosyltransferase* (*GAUT)* and *UDP-glucose-4-epimerase* (*UGE)*), indicating a high carbon sink for pectin (Table 2), as can be seen in the fractionation process in which this class of polysaccharides is half of the *S. polyrhiza* cell wall (Fig. 2 and Table 1). The transcript level of *SpAXS*, which encodes the enzyme responsible for apiose biosynthesis, was 1.8 times lower than another pectin-related gene (*SpGAUT1)*, while apiose was one of the most significant neutral monosaccharides found in the *S. polyrhiza* cell wall (Tables 2 and 1).

It was evaluated the expression of twelve genes related to hemicellulose biosynthesis pathways. Genes mainly related to xyloglucan, xylan, and mannan biosynthesis are found in the medium and low categories (Table 2). A glucomannan synthesis transcript was the second most highly expressed among the evaluated transcripts (*glucomannan-4-β-mannosyltransferase* – *SpCSLA* – 1.3) (Table 2).

Monosaccharide Variation in S. polyrhyza Cell Wall Under Distinct Cultivation and Hydrolysis Methods

S. polyrhiza 9509 grown under the same conditions at different developmental stages may have quantitative variation in the monosaccharide levels (Supplemental Table 5). Therefore, the AIR composition of published works and internal lab data for the species was evaluated. The recovered data was normalized, and the growth media, microclimate conditions, time of cultivation, and hydrolysis method were considered for comparison. The normalized monosaccharide levels were consistent and reveal a cell wall characterization of 20.6% (± 1.9) galactose, 17.4% (± 1.1) arabinose, 15.5% (± 1.1) xylose, 21.9% (± 2.9) apiose, 5.4% (± 1.7) mannose, 7.5% (± 0.6) rhamnose, 9.3% (± 1.9) glucose, and 2.4% (± 0.2) fucose (Supplemental Table 5).

Discussion

The NDP-sugar pathways directly relate to the carbon flux from photosynthesis with the hexoses-phosphate distribution to synthesize the cell wall, soluble sugars, and starch [13]. Besides, critical points of the pentoses-phosphate, involved in synthesizing organic acids, nucleotides, amino acids, lignin, and polyphenols, interconnect with these pathways [16]. Therefore, understanding the NDP-sugar pathways enlightens the plant metabolism in its essential function in growth, directly impacting biomass accumulation. In this study, the genes related to the carbohydrate metabolism that leads to the cell wall's formation were retrieved. Some transcripts levels were correlated to the chemical features of the giant duckweed, *S. polyrhiza*. In addition, other related studies were performed, as the transcriptomic analysis of *Landoltia punctata* under nutrient starvation [17], *S. polyrhiza* 7498 under abscisic acid treatment [18], and some *Lemna* studies under different treatments [19]. However, most of the data are not available in public databases. The only available RNA-seq data from *S. polyrhiza* was obtained from a response to treatment that induces the turion formation (dormancy state), which is known to be lower and distinct in *S. polyrhiza* strain 9509 [20]. However, even with these transcript databases defined for duckweeds, exploring these data to apply bioenergy is poorly unexplored.

S. polyrhiza 9509 has a genome of 138.6 Mbp distributed in 20 chromosomes, hosting 18,507 predicted genes. This genome has low heterozygosis, low methylation levels, and low contents of non-essential proteins, transposons, rDNA, and long terminal repeats [20]. A set of 190 genes related to known reactions that lead to cell wall polysaccharides synthesis in plants (mainly NDP-sugars) were searched and mapped onto the chromosomes of *S. polyrhiza*. The NDP-sugar-related genes were clustered in groups on different chromosomes according to the pathways that lead to the formation of non-structural carbohydrates (starch and sucrose), pectins, hemicelluloses, and cellulose. Clustering-like patterns were detected in categories of "sucrose metabolism," "pectins," and "hemicelluloses." However, for starch and cellulose, the distribution appears to be more arbitrary.

Cellulose's cell wall core is synthesized on the plasma membrane by cellulose synthases (CESA; EC 2.4.1.12) complexes [16]. In *S. polyrhiza* gene screening, here, 23 *CESA* genes (Fig. 4) distributed among 13 chromosomes (1,4,7–11,13,15,17–20) (Figs. 3 and 4) were identified. Cellulose is composed of β-1,4-D-glucose chains that, in *S. polyrhiza*, represent only 13% of the cell wall (Fig. 2 and Table 1). This data confirms previous reports [8]. However, some studies reported duckweed with cellulose contents ranging from 25 to 55% [21, 22], suggesting that cellulose contents may vary up to fivefold. This polymer displays some recalcitrance to hydrolysis, which interferes with biofuel production, but could be bypassed by modifying cellulose crystallinity [23]. The low proportion of cellulose in duckweeds compared to the 40% found in land plants may indicate the higher importance of pectins and hemicelluloses for duckweed walls. The higher proportion of pentoses in duckweeds is due to the high levels of apiose and xylose (pectin and hemicellulose, respectively) (Table 1 and Supplemental Table 5). Also, their negative aspect for fermentation makes the increase of cellulose suitable for bioelectricity and bioenergy. However, for this purpose, a deep study in the multigenic family of *cellulose synthases* is needed to evaluate these polymer crosslinks within duckweeds. Despite detecting the scarcity of cellulose in *S. polyrhiza* cell walls and fully understanding of the applications of this polymer to bioenergy, more accurate analysis needs to be performed, focusing on this polysaccharide synthesis.

Pectins are responsible for holding together the cellulose-hemicellulose portions in the cell wall and are also found in the middle lamella, junction zone, xylem, and fiber cells [4]. Pectins are galacturonic acid–rich polysaccharides such as homogalacturonans (HG), rhamnogalacturonans (RG), apiogalacturonans (API), and xylogalacturonans (XGA) [4]. The pectin scaffold (α-1,4 linked galacturonic acids) is built from the derivation of UDP-glucuronate, which is synthesized by the oxidation of UDP-Glucose by UDP-glucose dehydrogenase (UGD; EC 1.1.1.22), followed by the epimerization to UDP-Galacturonate by UDP-Glucuronate-4-epimerase (GAE, EC 5.1.3.6) [24] (Fig. 1). Galacturonosyltransferase (GAUT; EC 2.4.1.43) catalyzes the transfer from UDP-Galacturonate to homogalacturonans acceptors, generating the polysaccharide chains [25]. Duckweed biomass is pectin-rich [6], and here it is reported that pectins represent 49% of the *S. polyrhiza* cell wall (Fig. 2 and Table 1). Some of these pectins are likely to be linked to the cellulose microfibrils since pectin monosaccharides (apiose and rhamnose) were found on the cellulose-containing residue fractions (Table 1), which corroborated to the reported by Ge et al. [8], Soda et al. [9], and Zhao et al. [5]. The high pectin (and pentoses) content and its possible interlinks to cellulose negatively impact bioethanol production from biomass due to the barrier to hydrolytic enzymes from accessing fermentable sugars. Lionetti et al. (2010) [26] found that the reduction of homogalacturonan's methyl esterification increased the saccharification efficiency of *Arabidopsis* biomass. Therefore, more pectinases should be employed in enzymatic cocktails to provide fermentable sugars for bioethanol production. Because duckweeds display proportionally high amounts of pectins, this group of plants could benefit from pectin modifications to reach higher

saccharification levels. However, it is essential to remember that duckweeds are aquatic plants and the pectins they synthesize are probably crucial for maintaining growth in this kind of environment. Thus, any strategy to decrease the proportion of pectin in duckweeds will need to consider their possible effects on growth.

UDP-glucuronate also serves as the substrate for the synthesis of UDP-Xylose and UDP-Apiose by UDP-glucuronate decarboxylase and UDP-apiose/UDP-xylose synthase (*UXS* and *AXS*, EC 4.1.1.35), which are required for the biosynthesis of the pectins xylogalacturonan and apiogalacturonan [27] (Fig. 1). UDP-Xylose also is a substrate for part of xyloglucan and xylans polymers. Xylogalacturonan and apiogalacturonan are derived from HG, substituting *O-3* or *O-2* and *O-3* linked with xylose and apiose, respectively [4]. These two pectin classes are the trade-off between Lemnoideae and Wolffioideae subfamilies of duckweed [28], highlighting this as an interesting point for analyzing duckweed cell wall plasticity [7]. The apiose represents 15.4% (49.8 μg mg^{-1}) of AIR, being the main monosaccharide found in ammonium oxalate (44.3 μg mg^{-1}) and sodium chlorite (12.2 μg mg^{-1}) fractions (Table 1), even with a low relative transcript expression of 0.76 (Table 2). Otherwise, xylose represents 16.1% (51.9 μg mg^{-1}) of AIR and 5.8% of the ammonium oxalate (6.2 μg mg^{-1}) and sodium chlorite (5.4 μg mg^{-1}) fractions (Table 1). The pentoses apiose and xylose are not fermentable by typical *Saccharomyces cerevisiae* [44]. Currently, genetically modified *S. cerevisiae* strains can ferment xylose [29] but still are not fully employed in industries. Therefore, high levels of apiose and xylose are not yet considered suitable for biofuel production. Taking depletion mutants of *A. thaliana AtUXS* as an example, it is possible to improve glucose release for saccharification by 18%, together with greater accessibility to xylan's enzymatic breakdown [30]. Xylan contributes to recalcitrance reduction by the polysaccharide length and arrangement with other cell wall polymers, consequently improving biofuel production [30]. On the other hand, apiose is essential for plant development [31]. In duckweeds, apiose is positively related to fast growth and negatively for starch accumulation [7]. Thus, reducing the apiose content hypothetically increases starch levels, which would be beneficial for first-generation bioethanol. The starch content in *S. polyrhiza* was 3.3% (Fig. 1). However, this non-structural carbohydrate modulation can be increased by up to 70% through alterations in growth conditions [32], with no need for biomolecular approaches.

Aiming at high-value cosmetics and drug delivery instead of biofuel, these potential applications of apiogalacturonan could be an alternative for biorefinery [14]. Furthermore, pectins are used as a gelling and stabilizing agent in the food and cosmetic industries. Besides, some pectin-related molecules can improve human health by reducing cancer [33], cholesterol, blood glucose levels [34], and stimulating the immune response [35]. Thus, apiogalacturonan properties should also be investigated for these alternative purposes, and as its biosynthesis is dependent on a single copy of the *S. polyrhiza* genome, molecular approaches should be interesting.

Fucose is a monosaccharide present in rhamnogalacturonan type-II (RG-II) and xyloglucan. It is derived from GDP-mannose by the action of GDP-mannose-4,6-dehydratase (GMD, EC 4.2.1.47) and GDP-mannose-3,5-epimerase-4-reductase (GER, EC 1.1.1.271) [36] (Fig. 1). Duckweeds display a small proportion of fucosylated polysaccharides (Table 2). However, this sugar is essential for RG-II's maintenance and growth [37]. RG-II is the most complex pectin subclass of cell wall polysaccharides, containing an α-1,4-galacturonic acid backbone with several side branches consisting of 12 sugars and over 20 linkages [4]. Otherwise, RG-I consists of a backbone repeat of $[\alpha\text{-D-galacturonic acid-1–2-}\alpha\text{-1-rhamnose-1,4}]_n$ with side chains of α-L-arabinose *f* and β-D-galactose residues linked to the rhamnosyl sugars units [4]. Rhamnose is an exclusive sugar from rhamnogalacturonan. It is synthesized from UDP-Rhamnose through a three-stage reaction involving dehydration, epimerization, and reduction of UDP-Glucose into UDP-Rhamnose by UDP-glucose-4,6-epimerase (RHM, EC. 4.2.1.76) [37] (Fig. 1). *SpRHM* relative expression level was *Medium* (0.91) (Table 2), and rhamnose represented 8.8% of the cell wall monosaccharides (28.36 μg mg^{-1} AIR—Table 1). *AtRHM1* overexpression also increased galactose content with a concomitant reduction of glucose in *Arabidopsis* [38]. Notwithstanding, the silencing of *AtRHM1* did not alter the cell wall pattern [38], which may not impact biofuel production. However, a mutation on the *RHM* gene in *A. thaliana* suppressed *leucine-rich repeat extensin* (*Irx*) genes that alter root hair formation [39] and also rhamnose-polysaccharides coordinated some helical distribution of leaves during plant growth [40]. Therefore, altering the *RHM* gene in *S. polyrhiza* would probably change frond (leaf) morphology and affect plant development. Rhamnose is widely used in cosmetics, and it may also be responsible for anti-inflammatory, antiviral, and anti-cancer activity. Thus, rhamnose could also be a niche for applications through an *SpRHM* overexpression focusing on biorefinery.

UDP-Arabinose is the only NDP-sugar that is synthesized in the Golgi lumen in its pyranose (*p*) form by the epimerization of UDP-Xylose by UDP-arabinose-4-epimerase (UAE, EC 5.1.3.5) [15]. UDP-arabinopyranose (*p*) is transported to the cytosol for conversion in the furanose (*f*) form by UDP-arabinose mutase (UAM, EC 5.4.99.30) and then transported back to the Golgi lumen via UDP-Ara*f* transporters [41]. Arabinose is a hexose found in arabinans and as a branching of rhamnogalacturonans and xylans. Arabinans can be hydrolyzed by α-arabinofuranohydrolase (ASD, EC 2.7.1.52), and the free arabinose can be phosphorylated by

arabinokinase-1 (ARA1, EC 2.7.1.46) [42]. The biochemical evaluation of *S. polyrhiza* cell wall showed that arabinose constituted 17.3% of the AIR (56 μg mg^{-1} AIR) and was found mainly on the pectin-rich fractions (AmnOX—10.1 μg mg^{-1} and Chlorite—13.7 μg mg^{-1}) and 0.1 NaOH 1 M fractions (5.35 μg mg^{-1}) (part of hemicellulose fraction) (Table 1). Possibly, arabinose in *S. polyrhiza* is used to form arabinan chains. In addition, hemicellulosic arabinoses are responsible for biomass recalcitrance by interlinks with β-1,4-glucan [43]. Thus, the low incidence of hemicellulosic arabinose makes *S. polyrhiza* suitable for bioenergy purposes.

Hemicelluloses are polysaccharides containing β-1,4-pyranosyl glycosidic bonds in the main chain. They form heteromannans, xyloglucans, heteroxylans, and mixed-linkage glucan with different combinations of arabinose, mannose, xylose, fucose, and glucose monosaccharides [4]. As mentioned previously, xyloglucan is the main hemicellulose of duckweeds [6, 7]. This polysaccharide comprises repetitive units of four β-D-glycosyl residues, three of which contain α-D-xylosyl at the C-6 position, which can present in branches with galactose and fucose [14]. Thus, for its synthesis, the NDP-sugars UDP-glucose, UDP-fucose, UDP-galactose, and UDP-xylose are necessary. The UDP-galactose is formed directly from UDP-glucose through UDP-glucose-4-epimerase (UGE, EC 5.1.3.2) [44], and its phosphorylation can be catalyzed by UDP-glucose hexose 1-phosphate uridyltransferase (GALT, EC 2.7.7.12). The salvage pathway of galactose involves galactokinase (GALK, EC 2.7.16), which incorporates a phosphate into the free galactose [14] (Fig. 1). *UGE* can be considered a vital gene for xyloglucan synthesis (branching) and galactans [45]. The overexpression of *AtUGE2* in *A. thaliana* increased up to 80% of the cell wall galactose levels combined with *GalS1* (*galactan β-1,4-galactosyltransferase*), which is a potential source for fermentable sugar [45]. Zhang et al. [46] found a relationship between the lack of galactans with cellulose microfibrils orientation and plant growth interference on rice. Thus, galactans are needed for biomass accumulation. The galactose level in *S. polyrhiza* was 22% of the cell wall (74.8 μg mg^{-1} AIR—Table 1). The fractionation process demonstrated that the galactose was mainly galactans (AmnOx—17.4 μg mg^{-1}—Table 1) and secondarily as xyloglucans (0.1–4 M NaOH—Table 2). Therefore, overexpressing *SpUGE* could be favorable for biofuel production.

The heteromannans are the most ancient hemicellulose synthesized with the NDP-sugars GDP-Mannose, GDP-Glucose, and UDP-Galactose. The pathway for mannan synthesis depends directly on fructose-6-phosphate and involves the enzymes mannose-6-phosphate-isomerase (MPI, EC 5.3.1.8), phosphomannomutase (PMM, EC 5.4.2.8), and mannose-1-phosphate-guanylyltransferase (MGP, EC 2.7.7.13) [47]. Mannans can occur as linear chains of mannose that may be interspaced with glucose (glucomannan) and branched with galactose (galactomannan) [4]. Mannans represent 13.5% of the *S. polyrhiza* cell wall (43.9 μg mg^{-1} AIR—Table 1). A chemical linkage evaluation study determined that mannose in duckweed is found as glucomannan [6]. Due to this polymer's solubility, mannose is found mainly in ammonium oxalate (6.2 μg mg^{-1}) and sodium chlorite fractions (3.40 μg mg^{-1}) (Table 1). Besides that, the mannan-related transcripts *mannose-6-phosphate-isomerase* (*SpMPI*), *phosphomannomutase* (*SpPMM*), *mannose-1P-guanylyltransferase* (*SpMGP*), and *glucomannan-4β-mannosyltransferase (SpCSLA*) levels were the highest levels identified (Table 2). The pathway to mannan synthesis has a low number of gene copies, except for the *glucomannan synthase (MSR)* and *glucomannan-4β-mannosyltransferase (CSLA*) gene with 21 and 16 paralogs, respectively (Supplemental Table 1). Hence, the overexpression of the mannose precursors *mannose-6-phosphate-isomerase* (*MPI*), *phosphomannomutase* (*PMM*), and *mannose-1P-guanylyltransferase* (*MGP*), along with glycosyltransferases involved in this polysaccharide assembly, may increase the content of mannose in *S. polyrhiza* cell wall, which could make this plant a source for nutrition and human-health food supplement [36]. Additionally, mannose's high content for biofuel production could increase ethanol yield due to its relatively efficient fermentation by wild *S. cerevisiae* via the Embden-Meyerhoff pathway.

As fast-growing plants, duckweeds' distinct cell wall composition might be due to the clonal fragmentation and its growth and morphological responses to nutrient availability and population density [48]. The clonal propagation is related to the new fronds generated asexually, in which parental fronds can release up to twenty offspring, and these "daughter" fronds differ phenotypically [49]. The daughters' distinct phenotypes along with growth conditions and nutrient availability could impact the cell wall composition. Furthermore, it is known that biotic and abiotic stresses can alter cell wall composition and characteristics. Thus, a different phenotype makes sense for the cell wall in the offspring due to the change in the nutritional availability, the reflection of light, stalking, and shadow influence. Besides that, cell wall phenotype traits and proportions vary according to plant genotype [50]. The *S. polyrhiza* cell wall-AIR composition from previous studies has been compared with those obtained in this work and unpublished internal lab data. It is presented in Supplemental Table 5. The quantitative proportions of the sugars vary according to growth conditions (light intensity, photoperiod, temperature). However, when the data is normalized for comparative purposes of the percentages, a pattern emerges with 20.6% galactose, 17.4% arabinose, 15.5% xylose, 21.9% apiose, 5.4% mannose, 7.5% rhamnose, 9.3% glucose, and 2.4% fucose (Supplemental Table 5—heatmap average). Therefore, quantitative data

must be evaluated individually in each study, considering the plant growth conditions and the cell wall composition. The fermented sugars make up 60.7%, which is suitable for bioenergy applications.

Conclusion

S. polyrhiza starch synthesis, *de novo*, and *salvage* NDP-sugars pathways have few gene redundancies. This makes *S. polyrhiza* suitable for genetic modifications, promising biomass more ideal for bioenergy and biorefinery. However, any change in cell wall polymer proportions should be carefully planned to assess the trade-offs between the benefits for industry and the plant's growth capacity.

Supplementary Information The online version contains supplementary material available at https://doi.org/10.1007/s12155-021-10355-4.

Acknowledgements We thank Dr. Eny Iochevet Segal Floh for the use of laboratory facilities. We apologize to the colleagues whose work we were not able to cover or cite due to space limitations.

Author Contribution MSB, DP, AG, and EL planned the work. DP performed the biochemical analysis. BVN, DP, and MMZ did the bioinformatics work. AG, BNV, DP, and MSB analyzed the data. AG, BNV, DP, EL, and MSB wrote the manuscript.

Funding This work was supported by the Instituto Nacional de Ciência e Tecnologia do Bioetanol – INCT do Bioetanol (FAPESP 2014/50884–5 and CNPq 465319/2014–9). DP (CAPES 88882.377113/2019–1). AG (FAPESP 2019/13936–0). BVN (CAPES PNPD 20131621-33002010156P0). The support by a travel grant to EL by the U.S. Fulbright-Brazil Scholar Mobility Program (2014) to travel to the laboratory of MSB to jump-start this project in 2014–2015 is gratefully acknowledged. The authors thank the Fulbright Foundation for the fellowship to EL.

Declarations

Conflict of Interest The authors declare no competing interests.

References

1. Buckeridge MS (2017) The evolution of the Glycomic Codes of extracellular matrices. BioSystems 164:112–120. https://doi.org/10.1016/j.biosystems.2017.10.003
2. Carpita NC, Gibeaut DM (1993) Structural models of primary cell walls in flowering plants: consistency of molecular structure with the physical properties of the walls during growth. Plant J 3:1–30. https://doi.org/10.1111/j.1365-313X.1993.tb00007.x
3. Cosgrove DJ, Jarvis MC (2012) Comparative structure and biomechanics of plant primary and secondary cell walls. Front Plant Sci 3:204. https://doi.org/10.3389/fpls.2012.00204
4. Mohnen D, Bar-Peled M, Somerville C (2009) Cell wall polysaccharide synthesis. Wiley-Blackwell
5. Zhao X, Moates GK, Wellner N et al (2014) Chemical characterisation and analysis of the cell wall polysaccharides of duckweed *(Lemna minor)*. Carbohydr Polym 111:410–418. https://doi.org/10.1016/j.carbpol.2014.04.079
6. Sowinski EE, Gilbert S, Lam E et al (2019) Linkage structure of cell-wall polysaccharides from three duckweed species. Carbohydr Polym 223:115119. https://doi.org/10.1016/j.carbpol.2019.115119
7. Pagliuso D, Grandis A, Igarashi ESES et al (2018) Correlation of apiose levels and growth rates in duckweeds. Front Chem 6:1–10. https://doi.org/10.3389/fchem.2018.00291
8. Ge X, Zhang N, Phillips GC, Xu J (2012) Growing *Lemna minor* in agricultural wastewater and converting the duckweed biomass to ethanol. Bioresour Technol 124:485–488. https://doi.org/10.1016/j.biortech.2012.08.050
9. Soda S, Ohchi T, Piradee J et al (2015) Duckweed biomass as a renewable biorefinery feedstock: ethanol and succinate production from *Wolffia globosa*. Biomass Bioenerg 81:364–368. https://doi.org/10.1016/j.biombioe.2015.07.020
10. Popov SV, Günter EA, Markov PA et al (2006) Adjuvant effect of lemnan, pectic polysaccharide of callus culture of *Lemna minor* L. at oral administration. Immunopharmacol Immunotoxicol 28:141–152. https://doi.org/10.1080/08923970600626098
11. Filbry A, Siefken W, Breitenbach U, et al (2007) Cosmetic or dermatological preparations for skin care and cleaning, containing apiogalacturonan compounds or extracts thereof from seaweed, together with emulsifiers.
12. Cao HX, Fourounjian P, Wang W (2018) The importance and potential of duckweeds as a model and crop plant for biomass-based applications and beyond. In: Handbook of Environmental Materials Management. Springer International Publishing, pp 1–16
13. Verbančič J, Lunn JE, Stitt M, Persson S (2017) Carbon supply and the regulation of cell wall synthesis. Mol Plant 11:75–94. https://doi.org/10.1016/j.molp.2017.10.004
14. Bar-Peled M, O'Neill MA (2011) Plant nucleotide sugar formation, interconversion, and salvage by sugar recycling. Annu Rev Plant Biol 62:127–155. https://doi.org/10.1146/annurev-arplant-042110-103918
15. Seifert GJ (2004) Nucleotide sugar interconversions and cell wall biosynthesis: how to bring the inside to the outside. Curr Opin Plant Biol 7:277–284. https://doi.org/10.1016/j.pbi.2004.03.004
16. Carpita N, Tierney M, Campbell M (2001) Molecular biology of the plant cell wall: searching for the genes that define structure, architecture and dynamics. Plant Cell Walls 47:1–5. https://doi.org/10.1007/978-94-010-0668-2_1
17. Tao X, Fang Y, Xiao Y et al (2013) Comparative transcriptome analysis to investigate the high starch accumulation of duckweed *(Landoltia punctata)* under nutrient starvation. Biotechnol Biofuels 6:72. https://doi.org/10.1186/1754-6834-6-72
18. Wang W, Wu Y, Messing J (2014) RNA-Seq transcriptome analysis of *Spirodela* dormancy without reproduction. BMC Genomics 15:60. https://doi.org/10.1186/1471-2164-15-60
19. Yu C, Zhao X, Qi G et al (2017) Integrated analysis of transcriptome and metabolites reveals an essential role of metabolic flux in starch accumulation under nitrogen starvation in duckweed. Biotechnol Biofuels 10:167. https://doi.org/10.1186/s13068-017-0851-8
20. Michael TP, Bryant D, Gutierrez R et al (2017) Comprehensive definition of genome features in *Spirodela polyrhiza* by high-depth physical mapping and short-read DNA sequencing strategies. Plant J 89:617–635. https://doi.org/10.1111/tpj.13400
21. Longland JM, Fry SC, Trewavas AJ (1989) Developmental control of apiogalacturonan biosynthesis and UDP-apiose production in a duckweed. Plant Physiol 90:972–976. https://doi.org/10.1104/pp.90.3.972

22. Yadav D, Barbora L, Bora D, et al (2016) An assessment of duckweed as a potential lignocellulosic feedstock for biogas production. International Biodeterioration & Biodegradation An assessment of duckweed as a potential lignocellulosic feedstock for biogas production. https://doi.org/10.1016/j.ibiod.2016.09.007
23. Dadi AP, Schall CA, Varanasi S (2007) Mitigation of cellulose recalcitrance to enzymatic hydrolysis by ionic liquid pretreatment. In: Applied Biochemistry and Biotechnology. 407–421
24. Gu X, Bar-Peled M (2004) The biosynthesis of UDP-galacturonic acid in plants. Functional cloning and characterization of *Arabidopsis* UDP-D-glucuronic acid 4-epimerase. Plant Physiol 136:4256–4264. https://doi.org/10.1104/pp.104.052365
25. Sterling JD, Atmodjo MA, Inwood SE et al (2006) Functional identification of an *Arabidopsis* pectin biosynthetic homogalacturonan galacturonosyltransferase. Proc Natl Acad Sci U S A 103:5236–5241. https://doi.org/10.1073/pnas.0600120103
26. Lionetti V, Francocci F, Ferrari S et al (2010) Engineering the cell wall by reducing de-methyl-esterified homogalacturonan improves saccharification of plant tissues for bioconversion. Proc Natl Acad Sci 107:616–621. https://doi.org/10.1073/pnas.0907549107
27. Choi SH, Mansoorabadi SO, Liu YN et al (2012) Analysis of UDP-D-apiose/UDP-D-xylose synthase-catalyzed conversion of UDP-D-apiose phosphonate to UDP-D-xylose phosphonate: Implications for a retroaldol-aldol mechanism. J Am Chem Soc 134:13946–13949. https://doi.org/10.1021/ja305322x
28. Avci U, Peña MJ, O'Neill MA (2018) Changes in the abundance of cell wall apiogalacturonan and xylogalacturonan and conservation of rhamnogalacturonan II structure during the diversification of the Lemnoideae. Planta 247:953–971. https://doi.org/10.1007/s00425-017-2837-y
29. Moysés DN, Reis VCB, de Almeida JRM et al (2016) Xylose fermentation by *Saccharomyces cerevisiae*: Challenges and prospects. Int J Mol Sci 17:1–18. https://doi.org/10.3390/ijms17030207
30. Kuang B, Zhao X, Zhou C et al (2016) Role of UDP-glucuronic acid decarboxylase in xylan biosynthesis in *Arabidopsis*. Mol Plant 9:1119–1131. https://doi.org/10.1016/j.molp.2016.04.013
31. Zhao X, Ebert B, Zhang B, et al (2020) UDP-Api/UDP-Xyl synthases affect plant development by controlling the content of UDP-Api to regulate the RG-II-borate complex. Plant J 1–16. https://doi.org/10.1111/tpj.14921
32. Xiao Y, Fang Y, Jin Y et al (2013) Culturing duckweed in the field for starch accumulation. Ind Crops Prod 48:183–190. https://doi.org/10.1016/j.indcrop.2013.04.017
33. Leclere L, Cutsem P Van, Michiels C (2013) Anti-cancer activities of pH- or heat-modified pectin. Front Pharmacol 4 OCT:128. https://doi.org/10.3389/fphar.2013.00128
34. Jenkins DJA, Newton C, Leeds AR, Cummings JH (1975) Effect of pectin, guar gum, and wheat fibre on serum-cholesterol. Lancet 305:1116–1117. https://doi.org/10.1016/S0140-6736(75)92503-9
35. Popov SV, Ovodov YS (2013) Polypotency of the immunomodulatory effect of pectins. Biochem 78:823–835. https://doi.org/10.1134/s0006297913070134
36. Nakayama KI, Maeda Y, Jigami Y (2003) Interaction of GDP-4-keto-6-deoxymannose-3,5-epimerase-4-reductase with GDP-mannose-4,6-dehydratase stabilizes the enzyme activity for formation of GDP-fucose from GDP-mannose. Glycobiology 13:673–680. https://doi.org/10.1093/glycob/cwg099
37. Reiter WD, Vanzin GF (2001) Molecular genetics of nucleotide sugar interconversion pathways in plants. Plant Mol Biol 47:95–113. https://doi.org/10.1023/A:1010671129803
38. Wang J, Ji Q, Jiang L et al (2009) Overexpression of a cytosol-localized rhamnose biosynthesis protein encoded by *Arabidopsis* RHM1 gene increases rhamnose content in cell wall. Plant Physiol Biochem 47:86–93. https://doi.org/10.1016/j.plaphy.2008.10.011
39. Diet A, Link B, Seifert GJ et al (2006) The *Arabidopsis* root hair cell wall formation mutant lrx1 is suppressed by mutations in the RHM1 gene encoding a UDP-L-Rhamnose synthase. Plant Cell 18:1630–1641. https://doi.org/10.1105/tpc.105.038653
40. Saffer AM, Carpita NC, Irish VF (2017) Rhamnose-containing cell wall polymers suppress helical plant growth independently of microtubule orientation. Curr Biol 27:2248-2259.e4. https://doi.org/10.1016/j.cub.2017.06.032
41. Rautengarten C, Birdseye D, Pattathil S et al (2017) The elaborate route for UDP-arabinose delivery into the golgi of plants. Proc Natl Acad Sci U S A 114:4261–4266. https://doi.org/10.1073/pnas.1701894114
42. Behmüller R, Kavkova E, Düh S et al (2016) The role of arabinokinase in arabinose toxicity in plants. Plant J 87:376–390. https://doi.org/10.1111/tpj.13206
43. Li F, Zhang M, Guo K et al (2015) High-level hemicellulosic arabinose predominately affects lignocellulose crystallinity for genetically enhancing both plant lodging resistance and biomass enzymatic digestibility in rice mutants. Plant Biotechnol J 13:514–525. https://doi.org/10.1111/pbi.12276
44. Rösti J, Barton CJ, Albrecht S et al (2007) UDP-glucose 4-epimerase isoforms UGE2 and UGE4 cooperate in providing UDP-galactose for cell wall biosynthesis and growth of *Arabidopsis thaliana*. Plant Cell 19:1565–1579. https://doi.org/10.1105/tpc.106.049619
45. Gondolf VM, Stoppel R, Ebert B et al (2014) A gene stacking approach leads to engineered plants with highly increased galactan levels in *Arabidopsis*. BMC Plant Biol 14:344. https://doi.org/10.1186/s12870-014-0344-x
46. Zhang R, Hu H, Wang Y, et al (2020) A novel rice fragile culm 24 mutant encodes a UDP-glucose epimerase that affects cell wall properties and photosynthesis. J Exp Bot 1–14. https://doi.org/10.1093/jxb/eraa044
47. Bonin CP, Reiter W-D (2000) A bifunctional epimerase-reductase acts downstream of the MUR1 gene product and completes the de novo synthesis of GDP-L-fucose in *Arabidopsis*. Plant J 21:445–454. https://doi.org/10.1046/j.1365-313x.2000.00698.x
48. Zhang LM, Jin Y, Yao SM, et al (2020) Growth and morphological responses of duckweed to clonal fragmentation, nutrient availability, and population density. Front Plant Sci 11: https://doi.org/10.3389/fpls.2020.00618
49. Barks PM, Laird RA (2016) A multigenerational effect of parental age on offspring size but not fitness in common duckweed (*Lemna minor*). J Evol Biol 29:748–756. https://doi.org/10.1111/jeb.12823
50. Wood JA, Tan HT, Collins HM et al (2018) Genetic and environmental factors contribute to variation in cell wall composition in mature desi chickpea (*Cicer arietinum* L.) cotyledons. Plant Cell Environ 41:2195–2208. https://doi.org/10.1111/pce.13196